Presented at "Acoustical Imaging '82"
July 19-22, 1982 London

Ultrasonic Tomography for Differential Thermography

M. J. Haney and W. D. O'Brien, Jr.

Bioacoustics Research Laboratory
Department of Electrical Engineering
University of Illinois
1406 W. Green Street
Urbana, Illinois 61801 USA

INTRODUCTION

This paper describes work in progress in the study of ultrasound computer aided tomography (UCAT) and its application to differential thermography. There are many situations in which it is desirable to determine the amount of induced heating generated by applied hyperthermia (microwave or ultrasound). However, it is not always possible or safe to insert a temperature sensitive probe into the subject. The application of assessing tissue temperature from the temperature dependence of ultrasonic speed has been suggested by others (Bowen, et al., 1979; Nasoni, et al., 1979; Rajagopalan, et al., 1979). But it may be possible to refine the assessment of temperature change from the simultaneous determination of the acoustic speed and the ultrasonic attenuation coefficient. A method is outlined for producing maps of temperature change after heating.

Pulses of ultrasound are transmitted through the subject. Time of flight and frequency content measurements are made to analyze the speed of propagation and attenuation coefficient of the regions of the subject. Algebraic reconstruction, based on an interpolated model of the ray paths, is used to form transit time (inverse speed) and attenuation coefficient images. (An error

---

This research is funded in part by a grant from the National Institutes of Health (GM 24994), and by an unrestricted gift from Ultrasonic Research, Inc.

estimation is performed to be used in later analyses.) Differential images (before and after heating) are used to estimate temperature change.

EQUIPMENT

Our apparatus permits equiangle divergent beam data to be collected. Signals from a Perkin Elmer 7/32 computer are sent to a SYM-1 microcomputer, which in turn controls the positioning of two vertical posts in a water filled tank (see Figure 1). These posts trace out horizontal fan shaped sectors at arbitrary viewing angles.

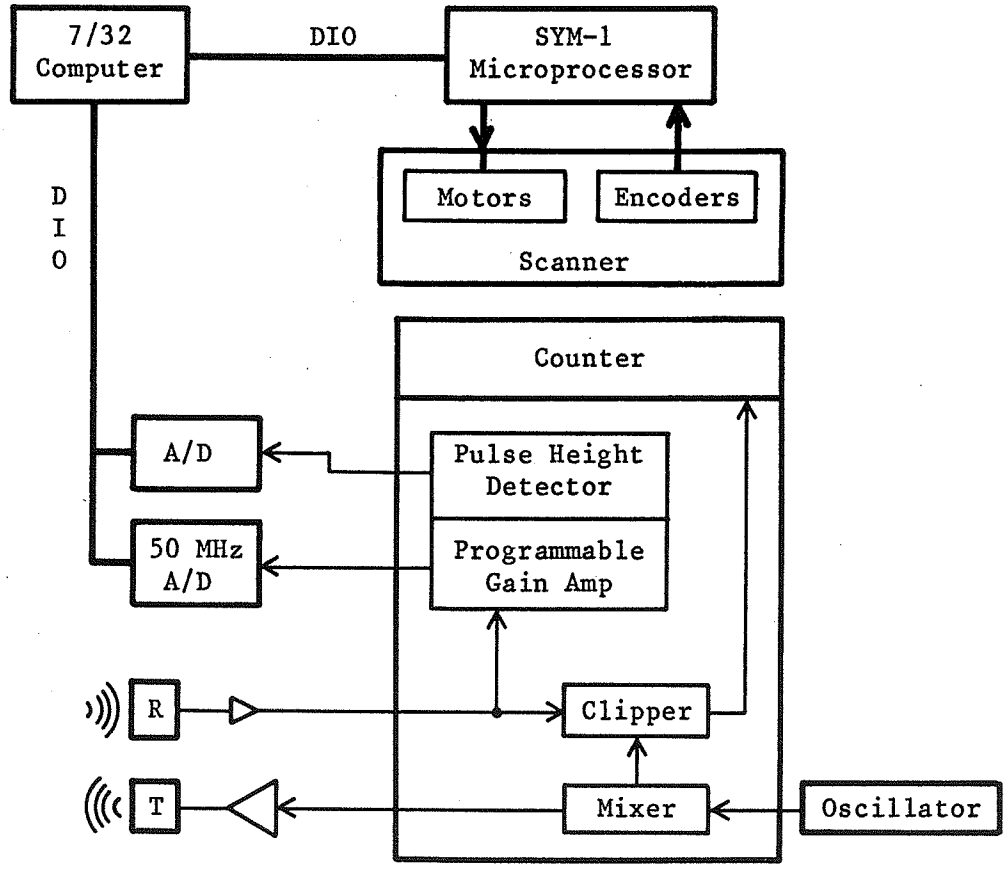

Figure 1: Equipment Block Diagram

A Hewlett-Packard 8660B Frequency Synthesizer supplies a reference signal (1 to 10 MHz) to a wave packet forming mixer (1/2 to 128 cycles). Pulses from this unit are amplified and fed to a Panametrics ultrasonic transducer mounted on one of the posts in

the tank. The other post holds a receiving transducer connected to a preamplifier and filters, then to a pulse height detector and time of flight counter (Hewlett-Packard 5328A Universal Counter). Two analog to digital converter are used to digitize the pulse height and the pulse itself. Samples are placed in the tank between to two transducers in a 20 cm diameter sample region.

METHODS

There are many alternatives in collecting ultrasound tomography data. Using threshold level detection, coarse time of flight measurements can be made. The received ultrasound pulse is digitized and recorded (8 bits @ 50 MHz) for fine time of flight and frequency content analyses.

The time of flight measurement represents the line integral of the transit times for the pulse through the intervening tissue. Tomographic reconstruction of this measurement yields the time per spatial resolution unit (inverse speed) of the tissue regions. Although one can normalize the time of flight with respect to the transit time through water, and thus reconstruct indices of refraction, the normalization would only have to be reversed in later stages of calculation. Note: the digitization of the received pulse allows for more accurate time of flight measurements by cross correlation methods (more accurate than threshold level detection).

Three methods are readily available for studying absorptive attenuation. The least accurate but most simple is to use narrow band pulses and measure the signal height within the received pulse. This method measures both absorption and scattering. Two more absorption sensitive (scattering insensitive) approaches are suggested by Kak (1979). By obtaining the frequency spectrum from the FFT of the received pulse, the attenuation can be determined by the ratio of spectral energies, or from the shift of the median frequency of the received pulse compared to a reference pulse transmitted through water. In all of the methods, the natural log of the attenuation gives the integral of the attenuation coefficient through the intervening tissue.

Reconstruction is based on an algebraic model of the physical system. Consider the time of flight per unit spatial resolution, or the attenuation coefficient, as a function $f(x,y)$. Then the measured data $g(\chi,\phi)$ for a divergent beam tomography system are given by

$$g(\chi,\phi)=\int f(x,y)ds \qquad [1]$$

Represented as a discrete sum,

$$g(\chi,\phi)=\sum\sum a(\chi,\phi;i,j)f(i,j) \qquad [2]$$

where $a(\chi,\phi;i,j)$ is the weight that $f(i,j)$ contributes to the (χ,ϕ) projection (see Figure 2).

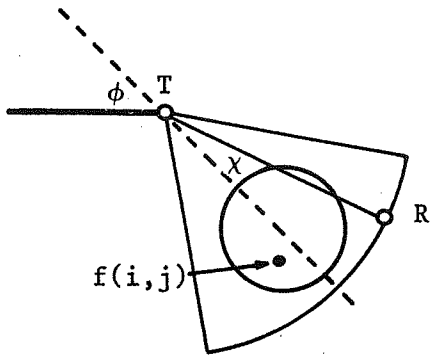

$$g(\chi,\phi)=\int f(x,y)ds$$

$$g(\chi,\phi)=\sum\sum a(\chi,\phi;i,j)f(i,j)$$

$$\tilde{g}=A\tilde{f}$$

Figure 2: Fan Beam Geometry

Most models assume $a(\chi,\phi;i,j)$ is equal to 0 or 1, or the length of the portion of the ray that passes through a box (pixel) around point (i,j) of the object (see Figure 3). These assumptions contribute a nontrivial amount of aliasing error in the name of computational conveniance. In analogy to one dimensional signal processing, these assumptions are equivalent to representing a function by a similar valued stairstep (piecewise constant) function.

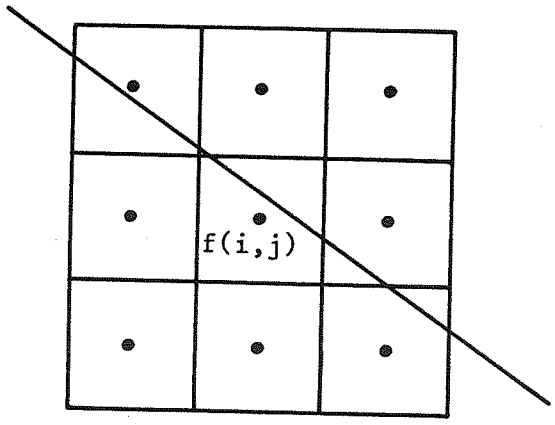

$$g(\chi,\phi)=\sum\sum \delta^{ij}_{\chi\phi} f(i,j)$$

$$g(\chi,\phi)=\sum\sum \delta^{ij}_{\chi\phi} L(i,j)f(i,j)$$

Figure 3: Conventional Models

Ideally, the contribution of each pixel should be calculated from the line integral of the function in that pixel. However, this would require an interpolation calculation involving every pixel in the image. Computationally, this would be very expensive.

A simple compromise is available through linear interpolation. For the region between any 4 sample points (e.g. (x,y) bounded by (i,j), (i+1,j), (i,j+1), and (i+1,j+1)):

$$f(x,y)=(i+1-x)(j+1-y)f(i,j) + (x-i)(j+1-y)f(i+1,j) + (i+1-x)(y-j)f(i,j+1) + (x-i)(y-j)f(i+1,j+1) \quad [3]$$

The line integral of the projection through this region can be evaluated explicitly. Assume the ray passes through the points (x0,y0) and (x0+Δx,y0+Δy), both on the edges of the region (see Figure 4). Then,

$$\begin{aligned}\int f(x,y)ds = {} & f(i,j)[\, L(i+1-x0)(j+1-y0) - L(i+1-x0)\Delta y/2 \\ & - L(j+1-y0)\Delta x/2 + L\Delta x\Delta y/3] \\ & + f(i+1,j)[\, L(x0-i)(j+1-y0) - L(x0-i)\Delta y/2 \\ & + L(j+1-y0)\Delta x/2 - L\Delta x\Delta y/3] \\ & + f(i,j+1)[\, L(i+1-x0)(yo-j) + L(i+1-x0)\Delta y/2 \\ & - L(y0-j)\Delta x/2 - L\Delta x\Delta y/3] \\ & + f(i+1,j+1)[\, L(x0-i)(y0-j) + L(x0-i)\Delta y/2 \\ & + L(y0-j)\Delta x/2 + L\Delta x\Delta y/3]\end{aligned} \quad [4]$$

where L is the euclidean length of the portion of the ray passing through the region.

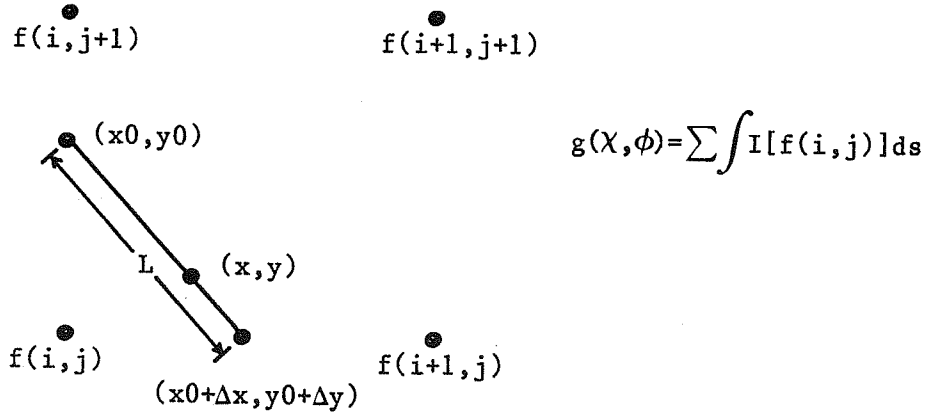

Figure 4: Proposed Linear Interpolation Model

Three notes are in order. First, although more involved, the calculation of $a(\chi,\phi;i,j)$ for interpolation can be performed once and saved, to be used for many reconstructions. Thus the computational expense is relatively unimportant. Second, in the previous assumptions, only a small proportion of the $a(\chi,\phi;i,j)$ are nonzero. In this integrated interpolation, only approximately twice as many values are nonzero. Thus sparse array data storage and processing methods can still be used. Finally, to compare to one dimensional signal processing, this interpolation is equivalent

to approximating a function by a similarly valued sawtooth (piecewise linear) function, with correspondingly less aliasing.

Using vector notation,

$$\tilde{g}=A\tilde{f}+\tilde{n} \qquad [5]$$

where $\tilde{n}$ represents the noise present in the collected data $\tilde{g}$. Reconstruction is preformed using the projection iterative method (Huang, 1977). Let g(m) be the m'th value of the vector $\tilde{g}$, and let $\tilde{a}(m)$ be a vector formed by the m'th row of A. Then the k+1 iteration is given by:

$$\tilde{f}^{k+1}=\tilde{f}^{k}+\frac{[g(m)-\tilde{f}^{k}\tilde{a}(m)]}{\tilde{a}(m)\tilde{a}(m)}\tilde{a}(m) \qquad [6]$$

where m = k modulo M (the number of values in $\tilde{g}$). After each M iterations, let

$$\tilde{n}=\tilde{g}-A\tilde{f}^{k} \qquad [7]$$

Termination of the iteration is controlled jointly by $\tilde{n}$ satisfying the statistics of the noise (measured independantly) and $\tilde{f}$ reaching a cyclic limit. Nonnegative value constraints and matrix order shuffling are used to improve the rate of convergence.

Algebraic reconstruction has been chosen for several reasons. First is flexibility. Missing data (data lost due to drop outs or rejected because of saturation) can be handled by simply eliminating rows of the A matrix. Second, uniformity of data collection is not required. Horn's theoretical approach (1977) requires reasonably continuous data. Davidson and Grunbaum's approach (1979) works for parallel beam data if all of the angles are known ahead of time. Thus run time difficulties (such as drop outs) result in large amounts of additional computation. Algebraic reconstruction works with what is available. Third, the majority of calculations involved are vector additions and dot products. The single instruction multiple data (SIMD) super computers of tomorrow will readily and efficiently handle such calculations. Finally, algebraic methods of reconstruction allow a better approach to estimating error.

Two error estimates are readily available by first computing the pseudo inverse matrix V for the matrix A (Hall, 1979). By rearranging the original vector equation,

$$\tilde{g}=A(\tilde{f}+\tilde{e}) \rightarrow V\tilde{g}-\tilde{f}=\tilde{e} \qquad [8]$$

From this, the error vector is given by $\tilde{e}=V\tilde{n}$. The second approach is a sensitivity analysis:

$$\sum \frac{f(i)}{g(j)} * \sigma^2 = V\tilde{\sigma}^2 = \tilde{\sigma}_f^2 \qquad [9]$$

where σ^2 is the varience of the through water sound measurements. A third method, suggested by Katz (1979), can be used, but it only estimates the total error over the entire image. This can be used to estimate the overall error in the temperature calculation, but a point by point error estimate is desired for later phases of the thermographic computations.

Temperature change estimation depends on the observation that the speed of propagation and attenuation coefficient are both temperature sensitive. For example, with water, the speed of propagation, measured in meters per second, can be approximated by c = 1403 + 5T + higher order terms (Kinsler and Frey, 1962), where T is measured in degrees celsius. Attenuation coefficients exhibit similar behavior (Fry and Dunn, 1962). Thus if one were to reconstruct a speed of propagation image c1(x,y) before heating, and another c2(x,y) after heating,

$$c1(x,y)-c2(x,y)=kc(x,y)\Delta T(x,y) \qquad [10]$$

where kc(x,y) is the thermal coefficient for the tissue at the point (x,y), and ΔT is the change in temperature. A similar calculation can be performed for attenuation images.

As a first approximation, setting kc(x,y) and ka(x,y) equal to the thermal coefficients for water will yield an estimate of differential temperature. A better estimate can be obtained by using those values of kc and ka available through the literature (Erikson, et al., 1974, or Goss, et al., 1978). Data available on the temperature dependence of the ultrasonic attenuation coefficient and the speed of sound in vivo are quite sparse. However, what is available, mostly in vitro, suggests that the speed of sound increases slowly with temperature in the range of 0.5 to 2 m/s per degree C around 40 degrees for non-fatty soft tissue (Bamber and Hill, 1979; Bowen, et al., 1979; Nasoni, et al., 1979; Rajagopalan, et al., 1979) and that the ultrasonic attenuation coefficient decreases slowly with temperature for some non-fatty tissues and increases for others with this dependence strongly dependent upon frequency and ambient temperature (Dunn and Brady, 1973 and 1974; O'Donnell, et al., 1977; Bamber and Hill, 1979). Thus, before the use of ultrasonic propagation property measurement can be used to assess tissue temperature change and related parameters, a much more detailed database must be obtained.

Given a table of thermal coefficients for common tissues, it is necessary to classify each point (x,y) according to its tissue type (liver, kidney, etc.), forming a map of the tissues conforming to the image. The easiest approach to this is to have a human

operator outline and identify the tissue regions from the reconstructed images. These outlines, with the identified tissues, form a classification map which directs the selection of kc and ka from the table of literature values. It is not necessary to classify every point of the image. Only the regions of interest need be identified.

ADDITIONAL STUDY

The final phase of this study will involve automated tissue region classification (instead of or in addition to operator specified tissue region classification) for assigning thermal coefficients. Parametric classification, based on the transit time and attenuation coefficient calculations, can be used to identify points of maximal confidence. Nonparametric (Bayesian) classification using an expected value - expected position model appropriate to the region being studied can also be used to identify points of high confidence. The error estimate plays an important role here, since it directly affects the confidence of the classification. Once these candidate points have been classified, constrained region growing can be used to classify neighboring points. Operator intervention in any of these steps would improve the results. Once a classification map has been generated, thermal coefficients can be assigned as described in the previous section.

REFERENCES

Bamber, J. C. and Hill, C. R., 1979, Ultrasonic attenuation and propagation speed in mammalian tissues as a function of temperature, Ultrasound in Medicine and Biology, vol. 5, no. 2, pp 149-157.

Bowen, T., Conner, W. G., Nasoni, R. L., Pifer, A. E., and Sholes, R. R., 1979, Measurement of the temperature dependence of the velocity of ultrasound in soft tissue, in: "Ultrasonic Tissue Characterization II," M. Linzer, ed., U.S. Government Printing Office, Washinton, D.C., NBS Special Publication 525, pp 57-61.

Davidson, M. E. and Grunbaum, F. A., 1979, Convolution algorithms for arbitrary projection angles, IEEE Trans. Nuclear Science, vol. NS-26, No. 2, pp 2670-2673.

Dunn, F. and Brady, J. K., 1973, Pogloshchenie ul'trazvyeka v biologicheskikh sredakh, Biofizika 18, 1063. Translation, 1974, Ultrasonic absorption in biological materials, Biophysics 18, 1128.

Dunn, F. and Brady, J. K., 1974, Temperature and frequency dependence of ultrasonic absorption in tissue, Proceedings 8th International Congress on Acoustics, vol. I, p 366c.

Erikson, K. R., Fry, F. J., and Jones, J. P., 1974, Ultrasound in medicine - a review, IEEE Trans. Sonics and Ultrasonics, vol. SU-21, no. 3, pp 144-169.

Fry, W. J. and Dunn, F., 1962, Ultrasound: analysis and experimental methods in biological research, in: "Physical Techniques in Biological Research," Academic Press, New York.

Goss, S. A., Johnston, R. L., and Dunn, F., 1978, Comprehensive compilation of empirical ultrasonic properties of mammalian tissue, J. Acoust. Soc. Am., 64, pp 423-457.

Hall, E. L., 1979, "Computer Image Processing and Recognition," Academic Press, New York.

Horn, B. K. P., 1978, Density reconstruction using arbitrary ray sampling schemes, Proc. IEEE, vol. 66, no. 5, pp 551-562.

Huang, T. S., 1977, Algebraic methods of image restoration, in: "Digital Image Processing and Analysis," J. C. Simon, and A. Rosenfeld, ed., Noordhoff, Leyden.

Kak, A. V., 1979, Computerized tomography with x-rays, emission, and ultrasound sources, Proc. IEEE, vol. 67, no. 9, pp 1245-1272.

Katz, M. B., 1978, Questions of uniqueness and resolution in reconstruction from projections, in: "Lecture Notes on Biomathematics," Springer-Verlag, New York.

Kinsler, L. E. and Frey, A. R., 1962, "Fundamentals of Acoustics," Wiley and Sons, Inc., New York.

Nasoni, R. L., Bowen, T., Conner, W. G., and Sholes, R. R., 1979, In vivo temperature dependence of ultrasound speed in tissue and its applications to noninvasive temperature monitoring, Ultrasonic Imaging, vol. 1, no. 1, pp 34-43.

Rajagopalan, B., Greenleaf, J. F., Thomas, P. J., Johnson, J. A., and Bahn, R. C., 1979, Variation of acoustic speed with temperature in various excised human tissues studied by ultrasound computerized tomography, in: "Ultrasound Tissue Charaterization," M. Linzer, ed., U.S. Government Printing Office, Washington, D.C., NBS Special Publication 525, pp 227-233.